Experimental Realization of High Transmittance THz 90°-Bend Waveguide Using EMXT Structure

Li-Ming Si, Yong Liu, Hong-Da Lu, Hou-Jun Sun, Xin Lv, and Weiren Zhu

***Abstract*— We present a high efficiency terahertz (THz) 90°-bend electromagnetic crystal (EMXT) waveguide using Si-based microelectromechanical systems technology. The 2-D EMXT consists of a periodical array of square-shaped gold rods (13 × 13 cells) deposited on a silicon substrate, and a 200-nm gold layer is further sputter-coated on the gold rod array. The dimension of each rod is $48 \times 48 \times 241$ μm^3, and the total size of the EMXT is $1756 \times 1756 \times 787$ μm^3. The 90°-bend waveguide is fabricated by removing three rows of rods from the EMXT. Through rigorous numerical simulation, it is found that transmittance higher than 90% are found in the whole range from 0.365 to 0.578 THz. The bending performance of the waveguide is further experimentally measured, where transmittance as high as 91.2% is observed at 0.5 THz. The proposed 90°-bend EMXT waveguide can be widely used for applications in THz circuit integrations and THz communications.**

***Index Terms*— Electromagnetic crystals (EMXT), 90°-bend waveguide, terahertz (THz).**

I. Introduction

TERAHERTZ (THz) frequencies ranged from 0.1 to 10 THz have attracted significant attention owing to the greatly increasing applications in sensing, imaging, radar, astronomy, chemistry, biology, communication, etc [1], [2]. However, there is still a lack of good THz functional devices because conventional naturally occurring materials are absorptive and do not respond well to THz electromagnetic spectrum, known as "THz gap" [3]–[5]. For instance, one of the main problems is the difficulty in THz waveguiding, since natural dielectrics and metals exhibit non-negligible absorption and dispersion throughout the THz frequency range [6]. In recent years, a number of different THz straight waveguides based on metal wires [6] or porous polymer [7] have been proposed for THz applications. However, effective guiding THz waves around a corner is quite a big challenge that has not been solved. The desire to further ameliorate THz functional devices with compact size and high efficiency needs novel materials and technologies.

Artificial electromagnetic metamaterials, which govern electromagnetic waves with their elements' configurations and arrangements rather than the compositions [8]–[12], such as negative refractive index metamaterials, zero index materials and electromagnetic crystals (EMXTs), have recently received much attention owing to their extraordinary properties not readily achievable in natural. Metamaterials with special THz response offer great promise for various THz applications, including sources [13], micro-cavities [14], switches [15], lasers [16], amplifiers [17], modulators [18], filters [19], splitters [20], couplers [21], waveguides and antennas [22], [23]. In particularly, periodically arranged EMXTs (also called photonic crystals if operating at optical frequencies) are widely used in manipulating electromagnetic waves because of their electromagnetic band gaps [24], [25].

Most recently, we introduced linear and tapered defects into the metallic EMXTs for applications of THz straight waveguide and H-plane horn antenna [22], [23] using microelectromechanical systems (MEMS) techniques. Based on these paper, we present the design, fabrication, and characterization of an EMXT-based THz 90°-bend waveguide with high transmission for the first time in this letter. Such 90°-bend waveguide is designed by removing partial unit cells from the metallic EMXT to form a 90° sharply chamfered bend waveguide. It is numerically revealed that high transmittance ($>90\%$) can be realized in the frequency range from 0.365 to 0.578 THz by using full-wave finite-element simulation (ANSYS HFSS). Experimental measurements further demonstrate the transmittance as high as 91.2% at 0.50 THz, in good agreement with simulations.

II. Structure and Numerical Design

The structure of the proposed EMXT-based THz 90°-bend waveguide is shown in Fig. 1(a), which is composed of a two-dimensional (2-D) defective EMXT with width W, length W, and height H. The EMXT, consisting of a periodic arrangement of square-shaped gold rod ($a \times a \times h$) with the lattice constant P, is fabricated on silicon backgroud coated with a 200 nm gold layer using MEMS technology. Fig 1(b) and 1(c) show the optical microscope images of the top and side

Manuscript received October 19, 2012; revised January 20, 2013; accepted January 30, 2013. Date of publication February 1, 2013; date of current version February 15, 2013. The work of L.-M. Si, Y. Liu, H.-D. Lu, H.-J. Sun, and X. Lv was supported in part by the National High-tech R&D Program of China under Grant 2012AA8123012 and in part by the National Program on Key Basic Research Project of China under Grant 2010CB327505. The work of W. Zhu was supported by Australian Research Council within the frame of the Discovery Grant scheme under Grant DP110100713.

L.-M. Si, Y. Liu, H.-D. Lu, H.-J. Sun, and X. Lv are with the Beijing Key Laboratory of Millimeter Wave and Terahertz Technology, Department of Electronic Engineering, School of Information and Electronics, Beijing Institute of Technology, Beijing 100081, China (e-mail: lms@bit.edu.cn; fatufo@bit.edu.cn; luhongda0751@bit.edu.cn; sunhoujun@bit.edu.cn; lvxin@bit.edu.cn).

W. Zhu is with the Advanced Computing and Simulation Laboratory (AcL), Department of Electrical and Computer Systems Engineering, Monash University, Clayton VIC 3800, Australia (e-mail: weiren.zhu@monash.edu).

Color versions of one or more of the figures in this letter are available online at http://ieeexplore.ieee.org.

Digital Object Identifier 10.1109/LPT.2013.2244878

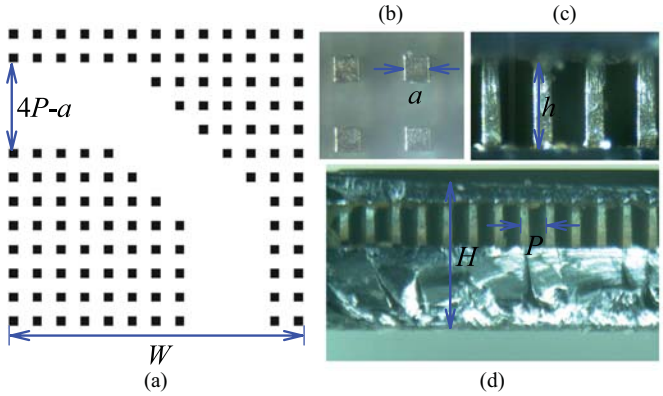

Fig. 1. (a) Schematic diagram of the EMXT-based THz 90°-bended waveguide, which is composed of square-shaped gold rods in the Si background; optical microscope image of the (b) top view and (c) side view of the EMXT structure, and (d) optical microscope image of the side view of the fabricated EMXT-based THz 90°-bended waveguide.

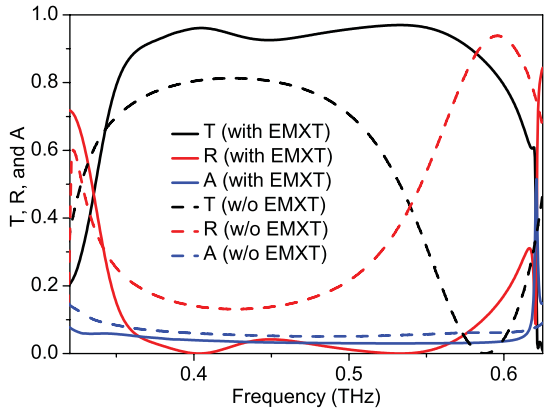

Fig. 2. Simulated transmittance T, reflectance R, and absorption A of the proposed EMXT-based THz 90°-bend waveguide (solid curves) and a same sized conventional 90°-bend waveguide without EMXT structure (dashed curves).

views of the fabricated EMXT. The 90°-bend waveguide is constructed by removing three rows of rods to form a 90° sharp chamfered bend structure as shown in Fig. 1(a). Two thick gold layers are cladded on the top and bottom of the final structure to restrict the electromagnetic waves inside the EMXT. The optical microscope image of the side view of the fabricated 90°-bended waveguide is shown in Fig. 1(d). The ideal geometrical dimensions are obtained by numerical parametric optimization: $W = 1756\ \mu$m, $H = 787\ \mu$m, $a = 48\ \mu$m, $h = 241\ \mu$m, $P = 132\ \mu$m.

In Fig. 2, we show the transmittance T, reflectance R, and absorption A of the proposed EMXT-based THz 90°-bend waveguide obtained from simulated scattering parameters, where $T = |S_{21}|^2$, $R = |S_{11}|^2$, and $A = 1 - |S_{11}|^2 - |S_{21}|^2$. To make a fair comparison, we also plot the simulated results of a same sized conventional 90°-bend waveguide (with out the EMXT structure) whose boundaries are supposed to be 200-nm gold layer. It is seen that the proposed EMXT-based THz 90°-bend waveguide has much higher transmittance and wider bending frequency band compared to the conventional 90°-bend waveguide. In particular, the proposed structure shows more than 90% transmittance from 0.365 to 0.578 THz, the relative bandwidth to the center frequency of which is as high as 45.2%, whilst the maximal transmittance of the conventional 90°-bend waveguide is only around 80%.

To illustrate the bending performance more colorfully, the mode patterns of the electric fields at 0.32 THz, 0.50 and 0.62 THz are investigated and compared in Fig. 3. For all these cases, the input waves are from the bottom entrance of the EMXT-based THz 90°-bend waveguide. When a 0.50 THz wave is input, Fig. 3(b) shows that the electromagnetic mode is well-confined inside the EMXT-based waveguide and bent smoothly to the horizontal direction. While for the cases of 0.32 and 0.62 THz, the electric fields are decreased through the 90°-bend waveguide and only little energy can be bent to the exit at the left side of the waveguide, as shown in Figs. 3(a) and 3(c). From these numerical simulations, we observed that such EMXT-based bending waveguide can support single mode at 0.5 THz. There is an alternative way to ascertain whether the proposed EMXT-based 90°-bend waveguide can operate single or multi-mode is by means of tracing the dispersion diagram. The mode patterns are in consistent with transmittance observed in Fig. 2.

III. Experimental Measurements

The high efficiency 90°-bend of the EMXT-based THz waveguide is further experimentally verified at 0.50 THz. The experimental set up is shown in Fig. 4, which is comprised of the three essential parts [22], [23]:

(1) A 0.50 THz transmitter based on an a 83.3 GHz millimetre wave source, a variable attenuator, a six-times frequency multiplier, and THz EMXT H-plane horn antenna with and without the 90°-bend waveguide under test.

(2) A 0.50 THz superheterodyne receiver composed of a standard diagonal horn antenna (Virginia Diodes Inc., VDI), a mixer (quasi optical heterodyne detection and local oscillator, the intermediate frequency (IF) and local oscillator (LO) frequencies are 6 GHz and 0.506 THz, respectively), a power meter, and a spectrum analyzer.

(3) An external ancillary systems including a mechanical servo system, a computer controlled terminal, and absorbing materials.

In our experiments, the transmit powers are measured through the THz EMXT H-plane horn antenna, which is fed by a standard rectangular waveguide (WR-1.9) with cross section size $483 \times 241\ \mu\text{m}^2$. The transmittance is determined by

$$T = 10^{(P_w - P_{wo})/10} \times 100\% \quad (1)$$

where P_w and P_{wo} represent the transmit IF powers with and without the 90°-bend waveguide, respectively. It is worth mentioning that the coupling loss in inter-connections may significantly affect the performance of THz circuits. To eliminate this influence, the impedance of the EMXT-based waveguide is optimized to well match with the feed line by rigorous full-wave simulations.

In Fig. 5 we show the measured IF power of the integrated antenna with and without the 90°-bend waveguide at H-plane radiation as a function of radiation angle θ. The results of experiments show that the measured error is less

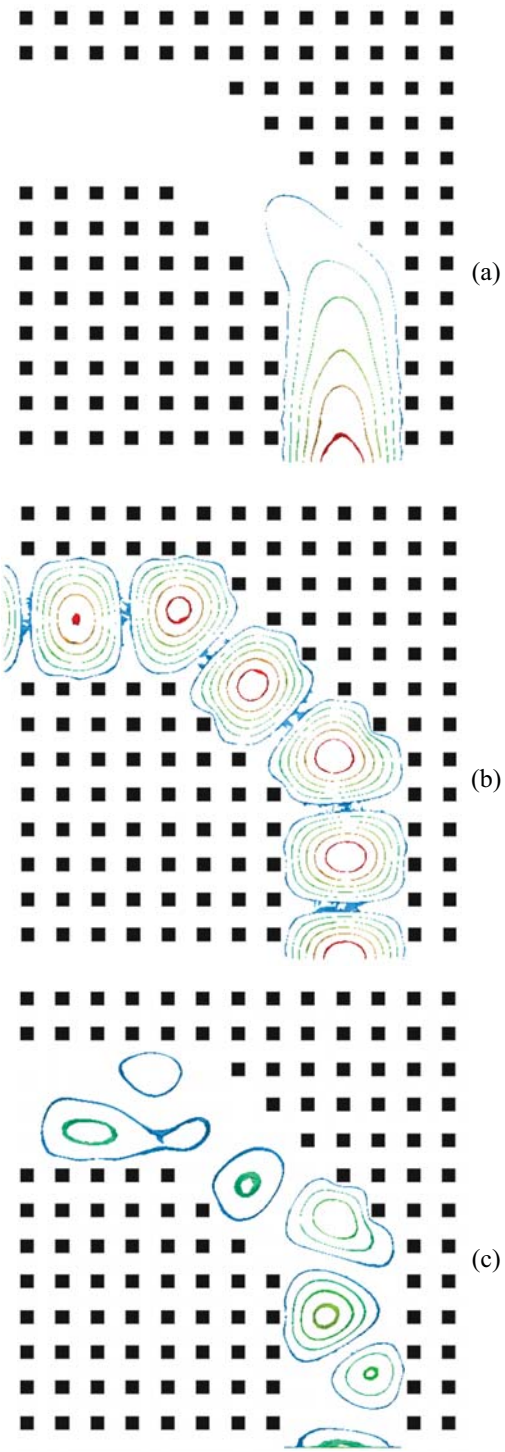

Fig. 3. Electric field amplitude patterns for the EMXT-based THz 90°-banded waveguide at (a) 0.32, (b) 0.50, and (c) 0.62 THz.

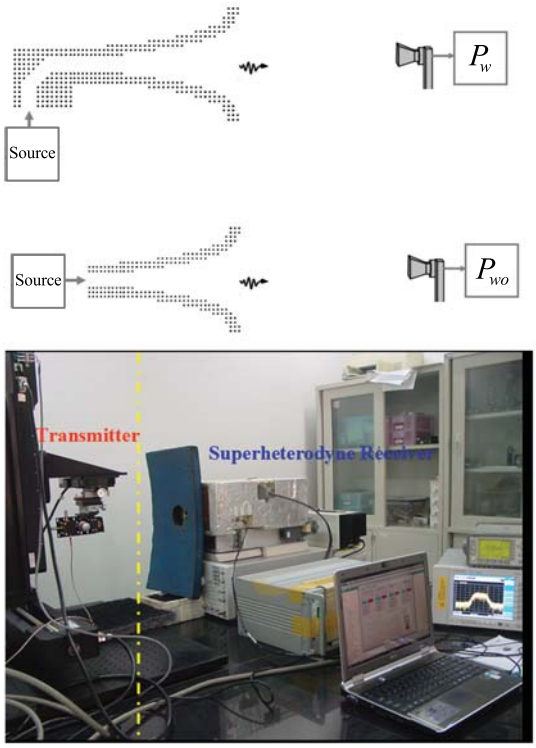

Fig. 4. Schematic diagram of the experiments for measuring the transmittance of the EMXT-based THz 90°-band waveguide. (a) P_w is measured with the H-plane horn antenna and the 90°-bend waveguide. (b) P_{wo} is measured with H-plane horn antenna only. (c) Experimental setup.

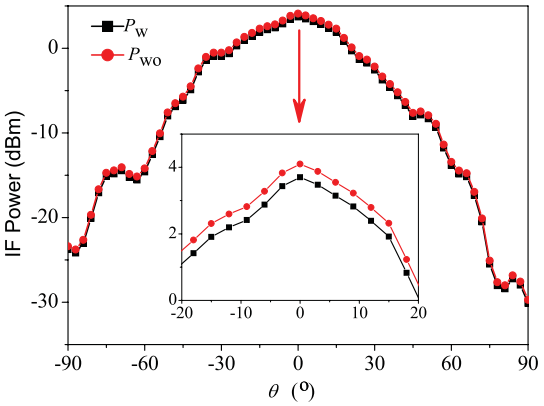

Fig. 5. Measured IF power of the integrated antenna with (P_w) and without (P_{wo}), the 90°-bend waveguide as a function of H-plane radiation angle θ. The insert shows the amplified view for θ close to zero.

than 0.3% for the proposed 90°-bend waveguide, which means the repeatability of the measurement is very good. It is seen that, the integration of 90°-bend waveguide does not affect the high directional radiation of the antenna, where main lobe gains are found to be 3.7 dBm and 4.1 dBm for the integrated antenna with and without the 90°-bend waveguide, respectively. Therefore, the measured transmittance of the EMXT-based THz 90°-bend waveguide is 91.2% at 0.50 THz calculated with Eq. (1), which agree reasonable well with the simulated transmittance of 95.5% by HFSS at this frequency. The measured transmittance is slightly lower than the simulated result which is likely due to the fabrication tolerances and surface roughness of the sputtered gold surface of the metallic cuboids and ground planes.

IV. Conclusion

We have experimentally proposed a high efficiency 90°-bend waveguide for THz frequency application. The 90°-bend waveguide was designed by removing three rows of unit cells in a THz EMXT composed of square-shaped gold

rod array. It was numerically shown that a broad-band high transmittance (> 90%) could be realized in the frequency range from 0.365 to 0.578 THz. Using MEMS technology, the practical bending waveguide was fabricated and measured at 0.50 THz. The measured transmittance of 91.2% is in good agreement with the simulated results. Our results reveal that the EMXT with certain THz frequency band gap can be used for effectively manipulating THz waves, which may find applications in practical THz communications and THz functional devices.

REFERENCES

[1] B. Ferguson and X. C. Zhang, "Materials for terahertz science and technology," *Nat. Mater.*, vol. 1, no. 1, pp. 26–33, Sep. 2002.

[2] P. H. Siegel, "Terahertz technology," *IEEE Trans. Microw. Theory Tech.*, vol. 50, no. 3, pp. 910–928, Mar. 2002.

[3] R. Kleiner, "Filling the THz gap," *Science*, vol. 318, pp. 1254–1255, Jun. 2007.

[4] M. Tonouchi, "Cutting-edge terahertz technology," *Nature Photon.*, vol. 1, pp. 97–105, Oct. 2007.

[5] L. M. Si and X. Lv, "Terahertz waves hairpin microstrip band-pass filter and its application to overlaid dielectric material detection," *Mod. Phys. Lett. B*, vol. 22, no. 29, pp. 2843–2848, Nov. 2008.

[6] K. L. Wang and D. M. Mittleman, "Metal wires for terahertz wave guiding," *Nature*, vol. 342, no. 7015, pp. 376–379, Nov. 2004.

[7] S. Atakaramians, *et al.*, "THz porous fibers: Design, fabrication and experimental characterization," *Opt. Express*, vol. 17, no. 16, pp. 14053–14062, Aug. 2009.

[8] G. V. Eleftheriades and K. G. Balmain, *Negative Refraction Metamaterials: Fundamental Principles and Applications*. Hoboken, NJ, USA: Wiley, 2005.

[9] W. Zhu, Y. Huang, I. D. Rukhlenko, G. Wen, and M. Premaratne, "Configurable metamaterial absorber with pseudo wideband spectrum," *Opt. Express*, vol. 20, no. 6, pp. 6616–6621, 2012.

[10] W. Zhu, I. D. Rukhlenko, and M. Premaratne, "Application of zero-index metamaterials for surface plasmon guiding," *Appl. Phys. Lett.*, vol. 102, no. 1, pp. 011910-1–011910-4, 2013.

[11] W. Zhu, I. D. Rukhlenko, and M. Premaratne, "Light amplification in zero-index metamaterial with gain inserts," *Appl. Phys. Lett.*, vol. 101, no. 3, pp. 031907-1–031907-4, 2012.

[12] L. M. Si, *et al.*, "Active microwave metamaterials incorporating ideal gain devices," *Materials*, vol. 4, no. 1, pp. 73–83, 2011.

[13] T. Chen, J. Sun, L. Li, J. Tang, and Y. Zhou, "Design of a photonic crystal waveguide for terahertz-wave difference frequency generation," *IEEE Photon. Technol. Lett.*, vol. 24, no. 11, pp. 921–923, Jun. 1, 2012.

[14] C. M. Yee and M. S. Sherwin, "High-Q terahertz microcavities in silicon photonic crystal slabs," *Appl. Phys. Lett.*, vol. 94, no. 15, p. 154104, Apr. 2009.

[15] J. Li, J. He, and Z. Hong, "Terahertz wave switch based on silicon photonic crystals," *Appl. Opt.*, vol. 46, no. 22, pp. 5034–5037, 2007.

[16] H. Zhang, L. A. Dunbar, G. Scalari, R. Houdre, and J. Faist, "Terahertz photonic crystal quantum cascade lasers," *Opt. Express*, vol. 15, no. 25, pp. 16818–16827, 2007.

[17] F. Liu, *et al.*, "Broadband terahertz pulses generated by a compact femtosecond photonic crystal fiber amplifier," *IEEE Photon. Technol. Lett.*, vol. 22, no. 11, pp. 814–816, Jun. 1, 2010.

[18] H. Chen, J. Su, J. Wang, and X. Zhao, "Optically-controlled high-speed terahertz wave modulator based on nonlinear photonic crystals," *Opt. Express*, vol. 19, no. 4, pp. 3599–3603, 2011.

[19] J. S. Li and S. Zouhdi, "Fano resonance filtering characteristic of high-resistivity silicon photonic crystal slab in terahertz region," *IEEE Photon. Technol. Lett.*, vol. 24, no. 8, pp. 625–627, Apr. 15, 2012.

[20] S. Li, H. W. Zhang, Q. Y. Wen, Y. Q. Song, W. W. Ling, and Y. X. Li, "Improved amplitude-frequency characteristics for T-splitter photonic crystal waveguides in terahertz regime," *Appl. Phys. B, Lasers Opt.*, vol. 95, no. 4, pp. 745–749, 2009.

[21] H. Kurt and D. S. Citrin, "A novel optical coupler design with graded-index photonic crystals," *IEEE Photon. Technol. Lett.*, vol. 19, no. 19, pp. 1532–1534, Oct. 1, 2007.

[22] L. M. Si, Y. Liu, S. Zhu, and H. Xin, "Integrated THz horn antenna using EBG structures," in *Proc. IEEE Int. Symp. Antennas Propag. USNC-URSI Nat. Radio Sci. Meeting*, Jan. 2011, paper A4-2.

[23] Y. Liu, L. M. Si, S. H. Zhu, and H. Xin, "Experimental realization of integrated THz electromagnetic crystals (EMXT) H-plane horn antenna," *Electron. Lett.*, vol. 47, pp. 80–82, Jan. 2011.

[24] T. Baba, "Slow light in photonic crystals," *Nature Photon.*, vol. 2, no. 8, pp. 465–473, 2008.

[25] J. D. Joannopoulos, P. R. Villeneuve, and S. Fan, "Photonic crystals: Putting a new twist on light," *Nature*, vol. 386, pp. 143–149, Mar. 1997.